Journal of Solid State Chemistry 183 (2010) 2274–2280

Contents lists available at ScienceDirect

Journal of Solid State Chemistry

journal homepage: www.elsevier.com/locate/jssc

Structural investigation of the Cu_2Se–In_2Se_3–Ga_2Se_3 phase diagram, X-ray photoemission and optical properties of the $Cu_{1-z}(In_{0.5}Ga_{0.5})_{1+z/3}Se_2$ compounds

M. Souilah, A. Lafond*, C. Guillot-Deudon, S. Harel, M. Evain

Institut des Matériaux Jean Rouxel (IMN), Université de Nantes, CNRS 2, rue de la Houssinière, BP 32229, 44322 Nantes Cedex 03, France

ARTICLE INFO

Article history:
Received 1 July 2010
Received in revised form
6 August 2010
Accepted 8 August 2010
Available online 13 August 2010

Keywords:
CIGSe
Crystal structure
XPS
Photovoltaic

ABSTRACT

Structures of compounds in the Cu_2Se–In_2Se_3–Ga_2Se_3 system have been investigated through X-ray diffraction. Single crystal structure studies for the so-called stoichiometric compounds $Cu(In,Ga)Se_2$ (CIGSe) confirm that the chalcopyrite structure (space group $I\bar{4}2d$) is very flexible and can adapt itself to the substitution of Ga for In. On the other hand a structure modification is evidenced in the $Cu_{1-z}(In_{0.5}Ga_{0.5})_{1+z/3}Se_2$ series when the copper vacancy ratio (z) increases; the chalcopyrite structure turns to a modified-stannite structure ($I\bar{4}2m$) when $z \geq 0.26$. There is a continuous evolution of the structure from $Cu_{0.74}(In_{0.5}Ga_{0.5})_{1.09}Se_2$ to $Cu_{0.25}(In_{0.5}Ga_{0.5})_{1.25}Se_2$ ((i.e. $Cu(In_{0.5}Ga_{0.5})_5Se_8$), including $Cu_{0.4}(In_{0.5}Ga_{0.5})_{1.2}Se_2$ (i.e. $Cu(In_{0.5}Ga_{0.5})_3Se_5$). From this single crystal structural investigation, it is definitively clear that no ordered vacancy compound exists in that series. X-ray photoemission spectroscopy study shows for the first time that the surface of powdered $Cu_{1-z}(In_{0.5}Ga_{0.5})_{1+z/3}Se_2$ compounds ($z \neq 0$) is more copper-poor than the bulk. The same result has often been observed on CIGSe thin films material for photovoltaic applications. In addition, optical band gaps of these non-stoichiometric compounds increase from 1.2 to 1.4 eV when z varies from 0 to 0.75.

1. Introduction

$Cu(In,Ga)Se_2$ compounds (CIGSe) have got a large importance as absorber materials in thin film solar cells. The chalcopyrite structure of $CuInSe_2$ has been determined by both powder and single-crystal X-ray diffraction (XRD) by several groups [1–3]. This structure (space group $I\bar{4}2d$) is derived from the cubic sphalerite ZnS structure in which two divalent atoms are replaced by both a monovalent Cu atom and a trivalent In atom. Because of the ordering of the cations, the unit cell doubles along the ***c*** direction, with a small tetragonal distortion ($c \approx 2a$). On the other hand, substitution of gallium for indium in $CuInSe_2$ increases the solar cell efficiencies. The corresponding compounds have the $CuIn_{1-x}Ga_xSe_2$ formulation and are claimed to form a solid solution series [4]. However, there are some discrepancies among the published results and, except for $CuInSe_2$ and $CuGaSe_2$, no single crystal structure determinations are available.

It is well known that the CIGSe compounds used as absorbers materials are often copper poor, i.e. the Cu/(In+Ga) ratio is less than 1 as it is in $Cu(In,Ga)Se_2$ [2,4–7]. Compositions such as $Cu(In,Ga)_3Se_5$ are evidenced at the surface of the CIGSe layer [8]. These so-called ordered vacancy compounds (OVC) have been investigated as bulk materials by powder diffraction [9–12] and it was noticed that the corresponding structures remain tetragonal with $c \approx 2a$.

This paper reports on structural investigations in the Cu_2Se–In_2Se_3–Ga_2Se_3 system from the stoichiometric to the very copper poor compounds, mainly based on single crystal X-ray diffraction technique. The main goal of this study is to understand how the CIGSe structure can adapt itself to the large difference in size between In^{3+} and Ga^{3+} as well as to the very large copper vacancy content. In addition, results of X-ray photoemission spectroscopy (XPS) on powdered samples are given.

2. Experimental

2.1. Synthesis and chemical analyses

The compounds were prepared by the solid state reaction of Cu, In, Ga, and Se in the appropriate ratios. The reactions were carried out in evacuated silica tubes heated at 1050 °C for several days. More details are given in a previous paper [13]. Bulk chemical compositions of the samples were analyzed by energy dispersive X-ray analysis (EDX) on polished sections of the products imbedded in epoxy. Elemental percentages were

* Corresponding author.
E-mail address: Alain.Lafond@cnrs-imn.fr (A. Lafond).

0022-4596/$ - see front matter © 2010 Elsevier Inc. All rights reserved.
doi:10.1016/j.jssc.2010.08.014

calculated using calibrated internal standards in order to obtain accurate and precise results. This method allows checking of homogeneity of the samples as well.

2.2. X-ray diffraction

The powder diffraction experiments were performed on a Bruker D8 diffractometer, equipped with a Ge(1 1 1) monochromator (Bragg–Brentano geometry, $\lambda=1.540598$ Å) and a Vantec position sensitive detector. Most of the powder patterns were recorded in the range 10-100° 2θ with 0.0084° 2θ-steps, either 0.3 s or 0.6 s per step. The samples were ground and passed through a 50 μm sieve before they were put into the sample holder. The Le Bail refinements were carried out with the help of the programs FullProf [14] and WinPlotr [15] using the pseudo-Voigt profile function.

For all the compounds, single crystal data collections were carried out on a Bruker-Nonius Kappa CCD diffractometer, using graphite monochromated Mo $K\alpha$ radiation (0.71073 Å). The experimental recording conditions were adapted depending mainly on crystal size. Although tetragonal symmetry was expected, the full diffraction sphere was recorded to ensure high redundancy and thus to obtain well-measured intensities. The recorded images were processed with the set of programs from Nonius. All the single crystal structure refinements have been done with the JANA2006 program [16]. For the stoichiometric compounds, single crystal structure refinements were performed for the nominal compositions of $x=0$, 0.25, 0.5, 0.75, and 1. For the $Cu_{1-z}(In_{0.5}Ga_{0.5})_{1+z/3}Se_2$ series, structure of compounds corresponding to $z=0.50$, 0.60, and 0.75 has been determined. In all cases, actual compositions of the single crystals have been checked by EDX analysis and have been found to be very close to those of the corresponding powders. Thus, unit cell parameters from the powders have been used for the structure refinements.

2.3. XPS and optical absorption measurements

X-ray photoemission measurements were performed on a Kratos Axis ultra spectrometer using a monochromatic Al $K\alpha$ X-ray source (1486.6 eV). The X-ray source ran at 150 W and the analyzed area was 700×300 μm^2. The pass energy was 160 eV for wide-scan spectra and 20 eV for valence band and core level. The energy scale was calibrated using Au $4f_{7/2}$ at 83.97 eV and Cu $2p_{3/2}$ peaks at 923.63 eV measured from sputter-cleaned Au and Cu films. Emission angle θ was kept constant and close to zero. The overall energy resolution, as determined using the Fermi edge of an Ag reference, was 0.47 ± 0.03 eV at 20 eV pass energy. The samples were ground and pressed into 6 mm diameter pellets and mounted on a double-sided carbon tape on an aluminum plate and transferred from the glove box to the XPS spectrometer using a case under argon.

Room-temperature UV–vis diffuse reflectance spectra were measured on a finely ground sample with a Cary 5G spectrometer (Varian) equipped with an integrating sphere. Diffuse reflectivity spectra were collected from 600 to 1600 nm (2.066–0.775 eV) with a 2-nm step and a recording time of 0.5 s/step using a Spectralon (from Labsphere) as the reference (100% reflectance). Absorption (K/S) was calculated from reflectivity using the Kubelka–Munk transformation $K/S=(1-R)^2/2R$, where R is the reflectivity, K the absorption coefficient, and S the scattering coefficient. In order to make comparison of the spectra easier, the data have been normalized between 0 and 1. Optical band gap is determined from a spectrum as the intersection point between the energy axis and the line extrapolated from the linear portion of absorption threshold.

3. Results

3.1. Compositional analyses

In the CIGSe compounds, charge balance is achieved with Cu^+, In^{3+}, Ga^{3+}, and Se^{2-}. Thus, in the copper poor compounds, one can expect a heterovalent substitution when three Cu^+ are replaced by one $(In,Ga)^{3+}$ with the formation of two vacancies on the copper site. Because the unit cell is barely affected by this substitution (the Se content remains 8 atoms/cell), the formula of CIGSe compounds is better written as $Cu_{1-z}(In_{1-x}Ga_x)_{1+z/3}Se_2$, where x and z stand for the Ga/(In+Ga) ratio and the copper deficiency ratio, respectively. With this formalism, the $Cu(In_{1-x}Ga_x)Se_2$ formula corresponds to $z=0$ and the $Cu(In_{1-x}Ga_x)_3Se_5$ formula can be rewritten as $Cu_{0.4}(In_{1-x}Ga_x)_{1.2}Se_2$, i.e. $z=0.6$.

Dispersion of individual spots analysis for each sample has been found to be quite low. Average compositions, close to those expected from the starting material stoichiometry, are plotted in the pseudo-triangular phase diagram Cu2Se–In2Se3–Ga2Se3 (see Fig. 1).

3.2. Crystal structure of stoichiometric compounds

The so-called stoichiometric compounds, with $CuIn_{1-x}Ga_xSe_2$ as a formula, are located on the line $z=0$ in Fig. 1. The evolution of unit cell parameters (Le Bail refinements) from composition $CuInSe_2$ ($x=0$) to $CuGaSe_2$ ($x=1$), given in Table 1, shows that the $CuIn_{1-x}Ga_xSe_2$ series is a solid solution. The linear decrease of a and c parameters is consistent with the relative values of the In^{3+} (0.76 Å) and Ga^{3+} (0.61 Å) crystal radii [17]. This observation is very similar to that published by Lam and Shih [4]. It should be noted that the evolutions of a and c parameters correspond to a slight decrease of the $c/2a$ ratio (tetragonal distortion) from 1.005 to 0.981, for $x=0$ and $x=1$, respectively.

Because the chalcopyrite structure derives from that of the ZnS sphalerite, the single-crystal reflections can be divided into two sets. High intensity reflections come from the basic ZnS structure and low intensity reflections depend both on the distribution of the Cu, In and Ga atoms on the cationic sites and the small deviation of anion position compared to that deduced from the ZnS structure. Thus, a particular attention was paid to the measurement of these low intensity reflections. In addition, high

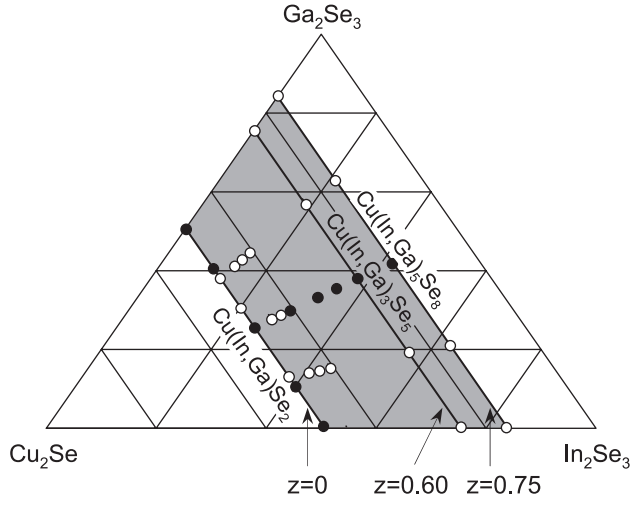

Fig. 1. Pseudo-ternary diagram in the Cu_2Se–In_2Se_3–Ga_2Se_3 system showing the composition of all synthesized compounds. Only the compounds corresponding to black circles are presented in this study.

Table 1
Main crystal data and structure refinement for $CuIn_{1-x}Ga_xSe_2$ (space group $I\bar{4}2d$).

# comp.	1	2	3[a]	4	5
x=Ga/(In+Ga)	0	0.21	0.48	0.82	1
a (Å)[b]	5.78361(8)	5.74784(6)	5.69700(4)	5.65010(5)	5.61911(9)
c (Å)[b]	11.6214(3)	11.5067(2)	11.33180(14)	11.14862(15)	11.0260(2)
N_{obs}/N_{all}(recorded)	4115/8578	4293/12,503	4204/10,648	3357/11,743	3726/12,095
R_{int}(obs/all)	5.39/5.45	6.50/7.77	5.49/5.72	6.28/7.71	6.37/7.04
# refined param.	11	12	12	12	11
N_{obs}/N_{all} (unique)	452/490	291/423	312/402	208/386	242/376
R(obs/all)	2.57/3.01	3.41/7.38	3.30/4.86	4.57/9.57	4.30/7.39
R_w(obs/all)	7.59/7.88	6.62/8.66	9.68/10.36	10.14/12.15	11.21/13.11
ρ (e^-/Å^3)+/−	0.99/−0.62	1.87/−1.94	1.22/−1.25	1.79/−1.88	1.64/−1.16
x (Se)	0.22738(10)	0.2334(4)	0.24000(19)	0.2472(2)	0.25062(13)
s.o.f. (Ga/In)	0/1	0.214/0.785(13)	0.482/0.518(11)	0.824/0.175(9)	1/0
d(Cu–Se) (Å)	2.4352(3)	2.4358(12)	2.4299(6)	2.4265(7)	2.4199(4)
d((In/Ga)–Se) (Å)	2.5859(3)	2.5460(13)	2.4958(6)	2.4449(7)	2.4159(4)
v(Cu)	0.94	0.94	0.95	0.96	0.98
v(Ga)		2.06	2.36	2.70	2.92
v(In)	2.92	3.26	3.73	4.28	
v(In,Ga)[c]	2.92	3.01	3.07	2.98	2.92

[a] From Ref. [13].
[b] From powder.
[c] v(In,Ga)=xv(Ga)+(1−x)v(In).

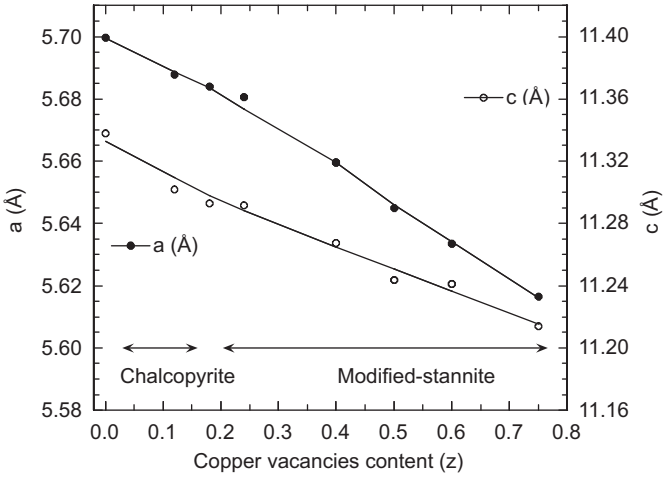

Fig. 2. Evolution of tetragonal unit cell parameters of the $Cu_{1-z}(In_{0.5}Ga_{0.5})_{1+z/3}Se_2$ series versus z.

sensitivity of the diffractometer allowed recording of at least 200 independent reflections ($\theta < 35°$, $-6 \le h \le 6$; $0 \le k \le 9$; $0 \le l \le 18$) for 11 or 12 refined parameters. Although the Cu^+ and Ga^{3+} atomic scattering factors are very close, thanks to the collection protocol, Cu^+ and Ga^{3+} can be distinguished during the structural refinements. No evidence was found for twinning on the (1 1 2) plane, which is usually observed for $CuInSe_2$ [18,19]. Refinement results are summarized in Table 1.

Bond valence sums have been calculated (see Table 1) according to the bond valence model of I.D. Brown, $v_{ij}=\exp((R_{ij}-d_{ij})/0.37)$, where R_{ij} is a tabulated value [20–22] corresponding to the $i-j$ chemical bond and d_{ij} is the actual bond distance between the atoms i and j.

3.3. *Crystal structure of the $Cu_{1-z}(In_{0.5}Ga_{0.5})_{1+z/3}Se_2$ compounds*

From the powder X-ray pattern, it is clear that all the $Cu_{1-z}(In_{0.5}Ga_{0.5})_{1+z/3}Se_2$ compounds adopt a tetragonal symmetry. Fig. 2 gives the evolution of a and c unit cell parameters as a function of copper deficiency ratio. When z increases, the unit cell parameters decrease because the structure contains more and more copper vacancies.

As was previously published [13], a structural modification occurs when the copper deficiency rises to 0.26, the standard chalcopyrite structure ($I\bar{4}2d$ space group) being replaced by a modified-stannite structure ($I\bar{4}2m$ space group). The main difference between the two structures comes from the cationic distribution. In the modified-stannite structure In^{3+} and Ga^{3+} are located on distinct crystallographic sites while these cations adopt the same positions in the chalcopyrite structure. Nevertheless, the structural evolution is quite small and does not affect the regular decreasing of unit cell parameters as is clearly evidenced in Fig. 2.

Crystal structure of the $Cu_{0.5}(In_{0.5}Ga_{0.5})_{1.17}Se_2$ compound has been determined through a single crystal diffraction experiment. The diffraction patterns obtained for all tested crystals could not be fully indexed in the standard tetragonal unit cell. A detailed analysis of the precession images (see Fig. 3) suggested that the crystals were twinned by reticular pseudo-merohedry [23]. Actually, the unit cell deduced from the powder analysis corresponds to a $c/2a$ ratio very close to 1. Thus the 3-fold [2 2 1] twinning direction used to index the whole pattern corresponds to the 3-fold [1 1 1] direction in the (**a**,**a**,**c**/2) cubic unit cell. In order to get all the reflections, a large unit cell (2**a**,2**a**,**c**) was used for integration of the collected images. The refinement was started with the structural model of $Cu_{0.74}(In_{0.5}Ga_{0.5})_{1.09}Se_2$ in the $I\bar{4}2m$ space group [13], for which the site occupancy factors are 2a(Cu) 87.5%, 2b(In) 100%, and 4d(Cu/Ga/In) 30.5%/54.3%/4.3%. In the case of $Cu_{0.5}(In_{0.5}Ga_{0.5})_{1.17}Se_2$, from the value of the atomic displacement parameter (ADP) it was clear that the site 2a was not 100% filled with Cu; consequently, a small fraction of copper remains on the 4d site. With Cu/Ga/In disorder and partial occupancy of two cationic sites, Se coordination is cell dependent. Consequently, averaging of the cell content gives rise to a large, non-harmonic distribution of Se electron density around the refined position. This particular distribution can be easily taken into account through a non-harmonic Gram–Charlier development of the atomic displacement parameter [24,25]. Indeed, introduction of third and fourth order Gram–Charlier non-harmonic atomic displacement parameters for Se position

significantly improved the refinement (lowering of residual R_{obs} value from 6.65 to 4.96), with a drop of the residues in the Fourier difference maps (maximum at 1.90 $e^-/Å^3$). The model is considered as valid since the negative part of electron densities around Se does not exceed, in absolute value, 1% of the probability density function maxima.

$I\bar{4}2m$ being a non-centrosymmetric space group, the absolute configuration was checked by refining the inversion twin ratio. The last step of the refinement leads to a quite good agreement factor $(R/R_w)_{obs}$ of 4.96 /11.25 for 1576 observed reflections ($\sin(\theta)/\lambda$ cut-off at 0.8) and 35 refined parameters. At this step, the Fourier-difference map is featureless.

It is worth noticing that all the selected single crystals corresponding to a composition with $z \geq 0.5$, including those with various gallium contents ($x \neq 0.5$), were found to be twinned. The refinement results for two other compounds of the series $x=0.5$ are given in Table 2.

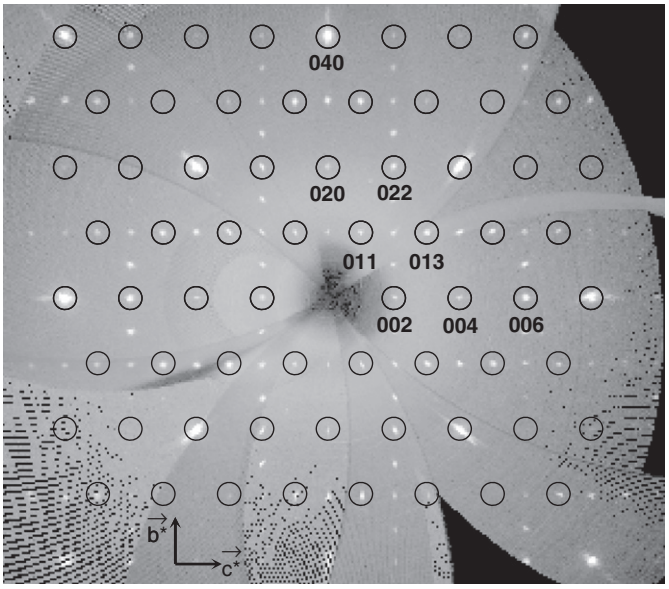

Fig. 3. Precession image of 0*kl* plane for the $Cu_{0.5}(In_{0.5}Ga_{0.5})_{1.17}Se_2$ compound. The indexed reflections (circles) correspond to the tetragonal unit cell ($a=5.6450$ Å and $c=11.2438$ Å) and the others are due to twinning along the [2 2 1] direction.

3.4. X-ray photoemission and optical properties of the $Cu_{1-z}(In_{0.5}Ga_{0.5})_{1+z/3}Se_2$ series

For all six compounds high resolution spectra of C1*s*, O1*s*, Cu $2p_{3/2}$, In 3*d*, Ga 2*p*, and Se 3*d* core levels on one hand, and valence band (VB) including Ga 3*p* and In 4*d*, on the other hand, were acquired. In addition the C 1*s* peak was used as an energy reference. Besides, intensity normalization was done based on the Se 3*d* peak because quantity of selenium is expected to be the same within the series. The spectra were integrated after subtraction of a Shirley background. The Cu $2p_{3/2}$ peak intensity shows a drastic decrease (roughly 50%) from stoichiometric $Cu(In_{0.5},Ga_{0.5})Se_2$ to $Cu_{0.88}(In_{0.5},Ga_{0.5})_{1.04}Se_2$ and remains roughly constant for greater *z* values (see Fig. 4). It is worth noticing that no major change in the In and Ga contents along the series can be observed.

The valence bands of $Cu_{1-z}(Ga_{0.5},In_{0.5})_{1+z/3}Se_2$ compounds (*z* varying from 0 to 0.75) are displayed in Fig. 5. First, one can notice that for all compounds the signal/noise ratio is high, which shows the cleanliness of the samples and, consequently, reliability of the measurements. Second, the valence band appears to be composed of two main contributions—regions A and B (see Fig. 5). For the stoichiometric compound ($z=0$), the valence band exhibits a high density of states at the top (region A), with two distinct structures (A1 and A2) of different intensities. When the material is copper-poor ($z=0.12$), the valence band undergoes a strong evolution with a drastic intensity decrease of the A region with A1 and A2 features of roughly same intensity. The $Cu_{0.88}(In_{0.5}Ga_{0.5})_{1.04}Se_2$ valence band maximum (VBM) shifts by about 0.3 eV towards higher binding energies. For $z \geq 0.12$ the A region energy range shrinks and the valence band maximum (VBM) shifts continuously with *z* towards higher binding energies, the higher binding energy side remaining at the same energy position. Intensity of the A region decreases slightly with an inversion of the A1 and A2 features. On the contrary, the B region

Table 2
Main crystal data for $Cu_{1-z}(In_{0.5}Ga_{0.5})_{1+z/3}Se_2$ compounds.

# comp.	3[a]	6[a]	7	8	9	10
z (from powder)	0	0.26	0.40	0.50	0.60	0.75
Space group	$I\bar{4}2d$	$I\bar{4}2m$	$I\bar{4}2m$	$I\bar{4}2m$	$I\bar{4}2m$	$I\bar{4}2m$
a (Å)[b]	5.69700(4)	5.6796(3)	5.6660(5)	5.6450 (5)	5.63351(13)	5.6166(7)
c (Å)[b]	11.33180(14)	11.2905(8)	11.2725(9)	11.2438(12)	11.2411(3)	11.214(11)
Twin?	No	No	Yes	Yes	Yes	Yes
N_{obs}/N_{all}(recorded)	4204/10,648	4403/12,705	7476/21,449	12,298/24,698	14,781/30,727	6423/10,235
R_{int}(obs/all)	5.49/5.72	7.78/9.29	8.32/11.45	6.77/7.09	6.25/6.66	5.68/5.86
# refined param.	12	16	23	35	25	35
N_{obs}/N_{all}(unique)	312/402	293/445	582/1121[c]	1576/1955	1517/1943	1098/1320
R(obs/all)	3.30/4.86	4.67/9.85	6.87/14.85	4.96/7.09	5.05/7.78	4.77/6.86
R_w(obs/all)	9.68/10.36	9.02/11.53	12.85/15.30	11.25/12.67	12.83/14.93	10.22/11.49
ρ +/− ($e^-/Å^3$)	1.22/−1.25	1.86/−2.31	1.70/−1.68	1.90/−1.36	1.56/−1.96	1.11/−1.33
x(Se)	0.24000(19)	0.2417(2)	0.2403(3)	0.2402(10)[d]	0.24058(12)	0.2378(5)[d]
z(Se)	0.125	0.12835(15)	0.12988(16)	0.130355(6)[d]	0.13033(7)	0.1317(9)[d]
2*a* s.o.f Cu Ga	–	0.875	0.851(4)	0.826(4)	0.8	0.5 0.253(−)
4*d* s.o.f Cu In Ga	–	0.305	0.174(−)	0.090(−)	0	0
		0.043	0.067(−)	0.083(−)	0.1	0.125(−)
		0.543	0.567(−)	0.583(−)	0.6	0.498(2)

[a] From Ref. [13].
[b] From powder.
[c] Due to the weak quality of the selected crystal a limit of $\sin(\theta)/\lambda \leq 0.75$ has been applied.
[d] For these structure refinements, the absolute configuration corresponds to $x(Se) \approx 0.76$ and $z(Se) \approx 0.87$. To make easy the comparison of selenium position the values $1-x$(Se) and $1-z$(Se) are indicated in the table.

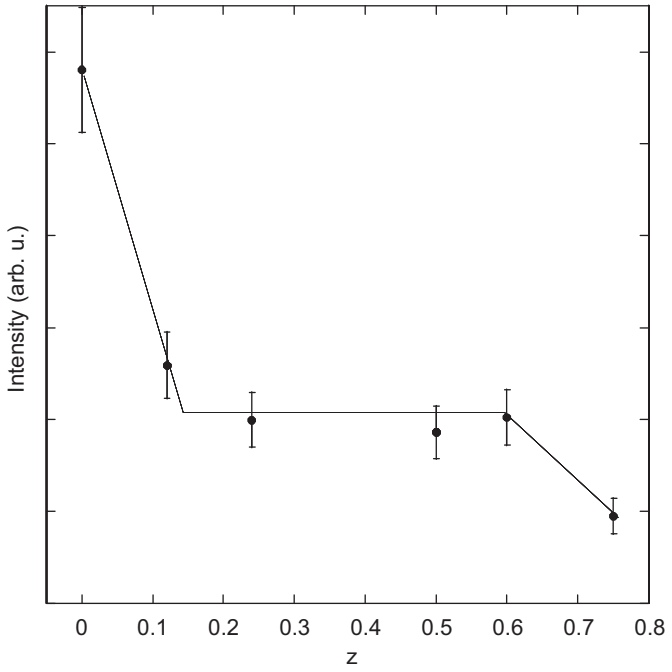

Fig. 4. Evolution of Cu $2p_{3/2}$ photoemission intensity as a function of z for the $Cu_{1-z}(In_{0.5}Ga_{0.5})_{1+z/3}Se_2$ series, indicating the drastic decrease of Cu-content at the surface (the solid line is a guide for the eyes).

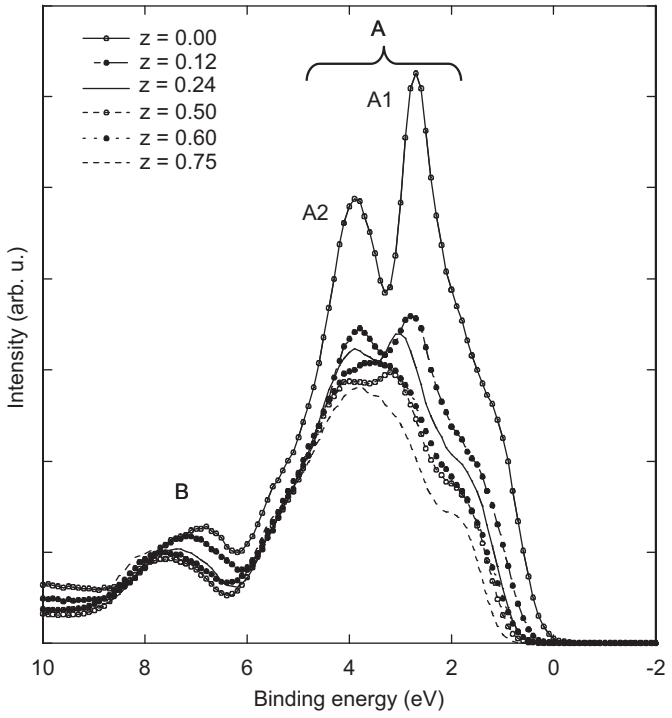

Fig. 5. Valence band photoemission spectra ($h\nu = 1486.6$ eV) for $z=0$ up to 0.75. The binding energy is referred to the E_F at BE=0 eV. The A region is mainly based on Se 4p and Cu 3d interactions while B corresponds to the In–Se band.

shows a much less spectacular evolution along the series. From $z=0$ to $z=0.24$ the maximum of the B region shifts towards higher binding energies and remains quite constant for $z \geq 0.40$.

The diffuse reflectance spectra for the $Cu_{1-z}(In_{0.5}Ga_{0.5})_{1+z/3}Se_2$ series are given in Fig. 6. It is clear that absorption thresholds shift towards higher energy when copper vacancy content increases.

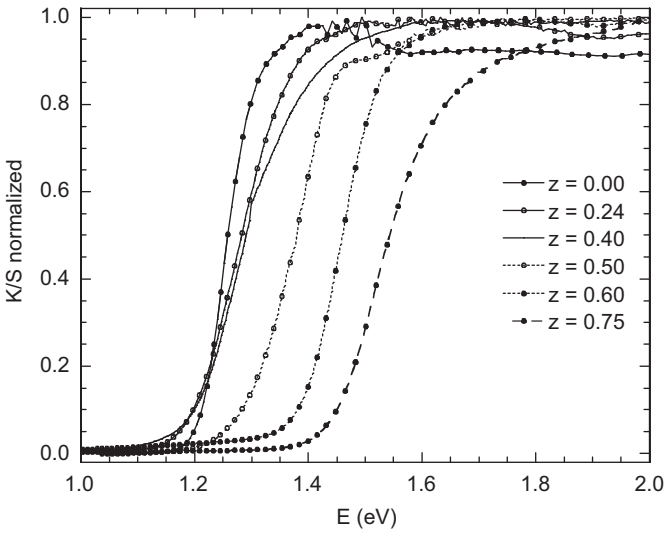

Fig. 6.. Evolution of Kubelka–Munk transformed diffuse reflectance versus energy for the $Cu_{1-z}(In_{0.5}Ga_{0.5})_{1+z/3}Se_2$ series, which indicates the increase of optical band gap when the copper vacancy ratio increases.

Because diffuse reflectance spectrum slightly depends on size of grains of the powder, the determination of band gaps is not very accurate. The band gap values of compounds with $z=0$, 0.24, and 0.40 are very close to 1.2 eV while they are equal to 1.29, 1.38, and 1.44 eV, for $z=0.50$, 0.60, and 0.75, respectively.

4. Discussion

The single crystal study of the stoichiometric compounds confirms previous studies done from powder diffraction. The chalcopyrite structure is found to be very flexible and can adapt itself to the replacement of the large In^{3+} by the small Ga^{3+} ion. This modification of average cationic radius is balanced by a slight displacement of selenium position (x,1/4,1/8) from x(Se)=0.22738(10) to 0.25149(6) for $CuInSe_2$ and $CuGaSe_2$, respectively. This variation is linear with the x=Ga/(In+Ga) gallium content and leads to a Cu bond valence quite constant and very close to 1 (see Table 1).

In literature, there are few results on structure of the high copper-poor compounds. Two structural models, based on the $P\bar{4}2c$ and $I\bar{4}2m$ space groups, have been proposed for $CuIn_3Se_5$ (i.e. $Cu_{0.4}In_{1.2}Se_2$) [9,26–28]. Most of these studies have been carried out from X-ray powder diffraction data and the correct space group for $CuIn_3Se_5$ is still under discussion. We have succeeded in selecting single crystals suitable for X-ray diffraction analyses showing a smooth evolution of structure for the compounds $Cu_{1-z}(In_{0.5}Ga_{0.5})_{1+z/3}Se_2$ from $z=0.5$ up to 0.75. All of these compounds adopt the modified-stannite structure with the $I\bar{4}2m$ space group, the cationic distribution on the crystallographic sites being adjusted only to the actual composition.

CIGSe compounds are well known to accommodate copper deficiencies for compositions in the vicinity of the stoichiometry 1:1:2 (i.e. Cu(In,Ga)Se_2). A very precise structural investigation of native defects in $CuInSe_2$ [29] has evidenced a slight under-stoichiometry for Se, which balances the copper vacancies. However, the present study shows that in high-copper-poor-gallium–indium compounds ($z>0.2$ and $x \neq 0$) the copper vacancies are balanced by an excess of the trivalent cations. In addition, there is a partial In–Ga segregation, indium being mainly on the 2b site of the $I\bar{4}2m$ space group. It seems that when copper vacancies appear in CIGSe compounds the structure is stabilized if

copper and gallium share the same crystallographic site (namely 4*d*). Thus, the structure changes from the chalcopyrite type ($I\bar{4}2d$) in which indium and gallium share the same atomic position to the lower symmetric space group $I\bar{4}2m$ in which the 2-fold sites (2*a* and 2*b*) allow a more flexible atomic distribution. In addition, since Cu^+ and Ga^{3+} cations have very close ionic radii, it is more realistic that these two cations share the same crystallographic position.

It is worth noticing that, according to this study, there is a continuous evolution of structure from $Cu_{0.76}(In_{0.5}Ga_{0.5})_{1.08}Se_2$ to $Cu_{0.25}(In_{0.5}Ga_{0.5})_{1.25}Se_2$, with no evidence of defined compounds for specific compositions or of the presence of ordered vacancies compounds in the case of $Cu_{0.4}(In_{0.5}Ga_{0.5})_{1.2}Se_2$ (i.e. $Cu(In_{0.5}Ga_{0.5})_3Se_5$) and $Cu_{0.25}(In_{0.5}Ga_{0.5})_{1.25}Se_2$ (i.e. $Cu(In_{0.5}Ga_{0.5})_5Se_8$) either. The same result has been obtained from single crystal structure determination of some very-copper-poor compounds with Ga/(In+Ga) ratio different from 0.5 (for example $Cu_{0.4}(In_{0.75}Ga_{0.25})_{1.2}Se_2$ and $Cu_{0.4}(In_{0.25}Ga_{0.75})_{1.2}Se_2$.

Let us now discuss the contribution of the XPS measurements to this study. According to previous studies [30,31], the regions labeled A and B are mainly based on Se 4*p* and Cu 3*d* interactions and on the In–Se band, respectively, whatever the chalcopyrite or stannite structure. Recently these attributions have been confirmed by ab-initio calculations [32]. Substitution of Cu^+ ions by M^{3+} ions affects the electronic structure with a strong reduction of the Se *p* character at the top of the valence band, due to the Cu vacancies. This result leads to a decrease of VB intensity, which is confirmed by the present XPS experiments (see Fig. 5). Moreover the drastic decrease of Cu $2p_{3/2}$ area, observed between $z=0$ and $z=0.12$, indicates that the surface of $Cu_{0.88}(In_{0.5}Ga_{0.5})_{1.04}Se_2$ compound is more Cu-poor than the bulk. Beyond this the area of this peak remains quite constant up to $z=0.60$, which means that in the 0.12-0.60 range, composition of the surface is roughly the same for these compounds. A quantitative analysis leads to a concentration ratio of Cu/(In+Ga) ≈ 0.3 close to that of the 1:3:5 compound. On the other hand, the A1 peak intensity of the VB continues to decrease regularly for those compounds. Due to the difference of inelastic mean free paths, information depth from VB is roughly twice larger than that of the Cu $2p_{3/2}$ core level. This explains that for $z=0.12$ to $z=0.6$, Cu $2p_{3/2}$ signals remain constant while the VB exhibits a slight continuous evolution. The presence of a Cu-depleted phase at the extreme surface of CIGSe compounds is well known in the case of CIGSe thin films and has been reported in numerous studies [8,33,34] but the nature and the depth extent of this Cu-depleted surface phase are still discussed [35–37].

The strong deviation of surface composition from bulk composition is observed for the first time on powdered samples elaborated through a process under equilibrium conditions. Although the studied powdered compounds do not have the same composition (in term of both copper and gallium contents) as that of the absorber films for photovoltaic application, Cu-depletion is probably a general phenomenon in CIGSe compounds.

This present study shows that in the solid solution series, stable CIGSe Cu-poor compounds exist in a wide composition range in terms of copper content. So the existence of a Cu-gradient below the surface seems to be a likely hypothesis. This gradient spreads probably from a nearly 1:3:5 phase up to the bulk composition for each studied powdered compound.

5. Conclusion

For the first time, an extensive crystal structure study of CIGSe compounds in a wide composition range, in terms of Ga/(In+Ga) as well as in terms of copper content, is presented. The main result is that there is a slight and continuous evolution of crystal structure when copper vacancy content increases. The space group changes from $I\bar{4}2d$ for high copper content to $I\bar{4}2m$ for copper-poor compounds corresponding to a small modification of cation distribution. In addition, for the studied compounds one can conclude that there is no vacancy ordering. On the other hand, this study shows that the experimental valence band is dramatically affected by increasing copper vacancy content. As it is observed for CIGSe thin film materials there is a segregation of the vacancies on the surface of the grains, leading to a composition close to $Cu_{0.4}(In_{0.5}Ga_{0.5})_{1.2}Se_2$ (i.e. $Cu(In_{0.5}Ga_{0.5})_3Se_5$). The increase of optical band gap from 1.2 eV for $Cu(In_{0.5}Ga_{0.5})Se_2$ to 1.4 eV for $Cu_{0.25}(In_{0.5}Ga_{0.5})_{1.25}Se_2$ is smaller than the measured VBM shift. Further investigations are in progress in order to determine the evolution of the conduction band.

This study confirms the high flexibility of the structure of CIGSe compounds, which are able to adapt themselves to substitution of Ga for In as well as to a wide range of copper vacancy content. This flexibility is probably related to the excellent behavior of these compounds as semiconductors in solar cells.

Appendix A. Supporting information

CIF files as supplementary data associated with this article can be found in the online version at doi:10.1016/j.jssc.2010.08.014.

References

[1] K.S. Knight, Mater. Res. Bull. 27 (1992) 161–167.
[2] J.M. Merino, J.L. Martin de Vidales, S. Mahanty, R. Diaz, F. Rueda, M. Leon, J. Appl. Phys. 80 (10) (1996) 5610–5916.
[3] W. Paszkowicz, R. Lewandowska, R. Bacewicz, J. Alloys Compd. 362 (2004) 241–247.
[4] W.W. Lam, I. Shih, Sol. Energy Mater. Sol. Cells 50 (1998) 111–117.
[5] G. Zahn, P. Paufler, Cryst. Res. Technol. 23 (4) (1988) 499–507.
[6] S.B. Zhang, S.H. Wei, A. Zunger, H. Katayama-Yoshida, Phys. Rev. B57 (16) (1998) 9642–9655.
[7] S.-H. Wei, S.B. Zhang, J. Phys. Chem. Solids 66 (2005) 1994–1999.
[8] D. Schmid, M. Ruckh, F. Grunwald, H.W. Schock, J. Appl. Phys. 73 (6) (1993) 2902–2909.
[9] W. Hönle, G. Kühn, U.-C. Boehnke, Cryst. Res. Technol. 23 (10–11) (1998) 1347–1354.
[10] N.S. Orlovaa, I.V. Bodnarb, T.L. Kushnerb, J. Phys. Chem. Solids 64 (2003) 1895–1899.
[11] S. Lehmann, D. Fuertes Marrón, M. Tovar, Y. Tomm, C. Wolf, S. Schorr, T. Schedel-Niedrig, E. Arushanov, M.C. Lux-Steiner, Phys. Status Solidi A 206 (5) (2009) 1009–1012.
[12] S. Lehmann, D. Fuertes Marrón, J.M. Merino, M. León, E.J. Friedrich, M. Tovar, Y. Tomm, C. Wolf, S. Schorr, T. Schedel-Niedrig, M.C. Lux-Steiner, Mater. Res. Soc. Symp. Proc. 1165 (2009) M03–09.
[13] M. Souilah, A. Lafond, N. Barreau, C. Guillot-Deudon, J. Kessler, Appl. Phys. Lett. 92 (2008) 2419231–2419233.
[14] J. Rodríguez-Carvajal, FullProf, 〈http://www.ill.eu/sites/fullprof/php/downloads.html〉, 2010.
[15] T. Roisnel, J. Rodriguez-Carvajal, Mater. Sci. Forum 378–381 (EPDIC 7,pt1) (2001) 118–123.
[16] V. Petricek, M. Dusek, L. Palatinus, Jana2006, in: The Crystallographic Computing System, Institute of Physics, Academy of Sciences of the Czech Republic, 2006.
[17] R.D. Shannon, Acta Crystallogr. A32 (1976) 751–767.
[18] J. Kessler, M. Bodegar, J. Hedström, L. Stolt, Sol. Energy Mater. Sol. Cells 67 (2001) 67–76.
[19] V. Lyahovitskaya, S. Richter, F. Frolow, L. Kaplan, Y. Manassen, K. Gartsman, D. Cahen, J. Cryst. Growth 197 (1999) 177–185.
[20] I.D. Brown, in: The Chemical Bond in Inorganic Chemistry: The Bond Valence Model, Oxford University Press, 2006.
[21] I.D. Brown, D. Altermatt, Acta Crystallogr. B41 (1985) 244–247.
[22] N.E. Brese, M. O'Keeffe, Acta Crystallogr. B47 (1991) 192–197.
[23] M. Nespolo, G. Ferraris, Acta Crystallogr. A60 (2004) 89–95.
[24] K.N. Trueblood, H.-B. Bürgi, H. Burzlaff, J.D. Dunitz, C.M. Gramaccioli, H. Schulz, U. Shmueli, S.C. Abrahams, Acta Crystallogr. A52 (1996) 770–781.

[25] L. Bindi, M. Evain, Am. Mineral. 92 (2007) 886–891.
[26] T. Hanada, A. Yamana, Y. Nakamura, O. Nittono, T. Wada, Jpn. J. Appl. Phys. 36 (1997) L1494–L1497.
[27] J.M. Merino, S. Mahanty, M. Leon, R. Diaz, F. Rueda, J.L. Martin de Vidales, Thin Solid Films 361–362 (2000) 70–73.
[28] J.M. Merino, M. Di Michiel, M. Leon, J. Phys. Chem. Solids 64 (2003) 1649–1652.
[29] L. Kaplan, G. Leitus, V. Lyakhovitskaya, F. Frolow, H. Hallak, A. Kvick, D. Cahen, Adv. Mater. 12 (5) (2000) 366–370.
[30] J.E. Jaffe, A. Zunger, Phys. Rev. B 28 (1983) 5822–5847.
[31] D. Schmid, M. Ruckh, H.W. Schock, Appl. Surf. Sci. 103 (1996) 409–429.
[32] M. Souilah, X. Rocquefelte, A. Lafond, C. Guillot-Deudon, J.-P. Morniroli, J. Kessler, Thin Solid Films 517 (2009) 2145–2148.
[33] E. Niemi, L. Stolt, Surf. Interface Anal. 15 (7) (1990) 422–426.
[34] A. Klein, J. Fritsche, W. Jaegermann, S.J.H.C. Kloc, E. Bucher, Appl. Surf. Sci. 166 (2000) 508–512.
[35] H. Mönig, C.-H. Fisher, R. Caballero, C.A. Kaufmann, N. Allsop, M. Gorgoi, R. Klenk, H.-W. Schock, S. Lehmann, M.C. Lux-Steiner, I. Lauermann, Acta Mater. 57 (2009) 3645–3651.
[36] D. Liao, A. Rockett, Appl. Phys. Lett. 82 (17) (2003) 2829–2831.
[37] T. Schulmeyer, R. Hunger, R. Fritsche, B. Jäckel, W. Jaegermann, A. Klein, R. Kniese, M. Powalla, Thin Solid Films 480–481 (2005) 110–117.